SCIENTIFIC REPORTS

OPEN

Calcium-deficient Hydroxyapatite as a Potential Sorbent for Strontium

Received: 6 December 2016
Accepted: 10 April 2017
Published online: 18 May 2017

Yurina Sekine[1], Ryuhei Motokawa[1], Naofumi Kozai[2], Toshihiko Ohnuki[2,3], Daiju Matsumura[1], Takuya Tsuji[1], Riku Kawasaki[4] & Kazunari Akiyoshi[4,5]

A calcium (Ca)-deficient hydroxyapatite was investigated for its potential to remove Sr^{2+} from environmentally relevant water. We conducted sorption tests on solutions containing magnesium ion (Mg^{2+}) and calcium ion (Ca^{2+}) as competing cations at a strontium ion (Sr^{2+}) concentration of 0.05 mmol/L. The Ca-deficient hydroxyapatite maintained a high Sr^{2+} sorption ratio of above 80% in the presence of Mg^{2+} and Ca^{2+} at the concentrations between 0.1 and 1.0 mmol/L, whereas the stoichiometric hydroxyapatite showed a lower ratio even in the presence of small amounts of Mg^{2+} and Ca^{2+} (72% for Mg^{2+} and 51% for Ca^{2+} at 0.1 mmol/L). For solutions with various Sr^{2+} concentrations between 0.01 and 10 mmol/L, Ca-deficient hydroxyapatite exhibited a higher Sr^{2+} sorption ratio than stoichiometric hydroxyapatite. The bonding states of Sr^{2+} on the Ca-deficient hydroxyapatite were evaluated by extended X-ray absorption fine structure measurements. The results indicated that there are specific sorption sites in Ca-deficient hydroxyapatite where Sr^{2+} is stably and preferentially immobilized.

Since the accident at the Fukushima-Daiichi nuclear power plant (FNPP) in 2011, there has been an immense need for novel ways to remove radioisotopes from contaminated water. A substantial number of radioisotopes such as strontium-90 (^{90}Sr), cesium-134 (^{134}Cs), and cesium-137 (^{137}Cs) were released from FNPP into the environment, thereby contaminating the seawater, groundwater, and land surface[1–3]. The radioactivity of the Sr and Cs released from FNPP onto the land surface was estimated to be around 8.56 PBq for ^{90}Sr and 288 PBq for ^{134}Cs and ^{137}Cs, whereas that of the strontium and cesium directly released into the ocean was estimated to be 52 GBq for ^{90}Sr and 3.5 PBq for ^{134}Cs and ^{137}Cs[4,5]. Of these radioisotopes, ^{90}Sr poses a major threat to human health and the environment because it can replace calcium (Ca) in bones and in plants, leading to genetic mutations[6]. Thus, studying the migration of ^{90}Sr in solution and determining suitable decontamination procedures are important issues to be researched.

Sorbent materials such as minerals[5,7–13] and polymeric materials[13] have been used for the removal of ^{90}Sr so far, however, development of a sorbent with both high sorption capacity and high ion selectivity is essential. Usually, several types of ion species such as magnesium ion (Mg^{2+}) and calcium ion (Ca^{2+}) are present in contaminated seawater and groundwater[5,14,15], making it difficult for sorbents to maintain their targeted ion sorption capacity. Sorbents with Cs^{+} selectivity have been developed[16,17], but materials with Sr selectivity have hardly been reported.

Hydroxyapatites (HAPs), which are calcium phosphate crystals, are the main components of our teeth and bones. They are of considerable interest in environmental and biomedical fields due to their ion-exchange ability and sorption capacity[5,12,18,19]. In HAP crystals, Ca^{2+} ions are located at two distinct crystallographic sites, which provide exchange sites for a wide range of divalent cations[20–22]. As Sr^{2+} and Ca^{2+} have the same charge and a similar ionic radii (1.2 Å[23] and 1.0 Å[23], respectively), Sr^{2+} can be adsorbed onto HAP with high efficiency[4,12,24].

[1]Materials Sciences Research Center, Japan Atomic Energy Agency, 2-4 Shirakata-Shirane, Naka-gun, Tokai, Irabaki, 319-1195, Japan. [2]Advanced Science Research Center, Japan Atomic Energy Agency, 2-4 Shirakata-Shirane, Naka-gun, Tokai, Ibaraki, 319-1195, Japan. [3]Laboratory for Advanced Nuclear Energy, Institute of Innovative Research, Tokyo Institute of Technology, Ookayama 2-12-1, Meguro, Tokyo, 152-8550, Japan. [4]Department of Polymer Chemistry, Graduate School of Engineering, Kyoto University, Katsura, Nishikyo-ku, Kyoto, 615-8510, Japan. [5]ERATO Bio-nanotransporter Project, Japan Science and Technology Agency, Kyoto University, Kastura, Nishikyo-ku, Kyoto, 615-8510, Japan. Correspondence and requests for materials should be addressed to Y.S. (email: sekine.yurina@jaea.go.jp)

	Ca/P ratio	Crystal size (nm)		Zeta potential (mV) at pH 7
		L^a	W^b	
DEF-HAP	1.38	43 ± 5.7 nm	17 ± 2.8 nm	−20.1
ST-HAP	1.68	89 ± 17 nm	17 ± 6.9 nm	−5.46

Table 1. Physical–chemical characterization of DEF-HAP and ST-HAP. [a]average length of the crystals. [b]average width of the crystals.

This preferential selectivity for Sr would make HAP an effective absorbent for the removal of Sr^{2+}. In fact, a HAP reactive barrier has already been successfully trialed at the Hanford nuclear site in the USA to prevent the migration of ^{90}Sr into the Columbia River[25]. Recently, HAPs are also being tested as a potential remediation material at the FNPP site[15].

The chemical composition of HAPs can be modified from the stoichiometric form ($Ca_{10}(PO_4)_6(OH)_2$) to the Ca-deficient form ($Ca_{10-x}(HPO_4)_x(PO_4)_{6-x}(OH)_{2-x}$) by selecting appropriate Ca/P molar ratios[18,26–28]. Natural HAPs in teeth and bones also have a nonstoichiometric form[18]. Moreover, HAPs can maintain their crystal structure regardless of the Ca/P molar ratio; thus, Ca-deficient HAP has vacant Ca^{2+} sites within its crystal structure[18,27,28]. It is known that the targeted ion-sorption properties of HAPs strongly depend on the Ca/P molar ratio[29–32]. In this study, we investigated the potential of Ca-deficient HAP for cleaning up contaminated water via Sr^{2+} sorption.

Results

Material characterization. The physical–chemical characterization of Ca-deficient hydroxyapatite (DEF-HAP, Ca/P = 1.38) and stoichiometric hydroxyapatite (ST-HAP, Ca/P = 1.68) is summarized in Table 1. Transmission electron microscopy (TEM) images of the materials (Fig. 1(a) and (b)) show that both DEF-HAP and ST-HAP form rod-like crystals and that the crystals of DEF-HAP are smaller than those of ST-HAP. The size of the crystals was estimated by analyzing these images; the average length (L) of the crystals of DEF-HAP (43 ± 5.7 nm) was approximately 46 nm shorter than that of ST-HAP (89 ± 17 nm), whereas their average widths (W) were almost identical (~17 nm) (Table 1). The X-ray powder diffraction (XRD) profiles of DEF-HAP and ST-HAP (Fig. 1(c)) have peaks in the 2θ range of 10–70°, and the positions of the peaks are similar to those of hydroxyapatites having a hexagonal structure ($P6_3/m$)[24]. The broader peak patterns observed for DEF-HAP might be due to its smaller crystal sizes, which agrees with the TEM observations. A broad band observed at a 2θ angle in the range 15°–28° might have originated from an amorphous component in the HAPs. Notably, the integrated intensities of the broad bands for DEF-HAP and ST-HAP are almost identical. At pH 7, the zeta potentials of DEF-HAP and ST-HAP were −20.1 and −5.46 mV, respectively.

Effect of competing cations. The effect of competing cations on the Sr^{2+} sorption capacity of DEF-HAP and ST-HAP was evaluated using an aqueous solution containing HAPs (35 mg), Sr^{2+} (0.05 mmol/L), and either Mg^{2+} or Ca^{2+} (0–50 mmol/L) in MilliQ water (7 mL). The solution was stirred for 5 h at pH 7. The supernatant was obtained by centrifugation and filtration, and the concentration of Sr^{2+} was determined using inductively coupled plasma-mass spectrometry (ICP-MS). Notably, the equilibrium time for the sorption was confirmed to be 1 h; hence, five hours were sufficient to evaluate the sorption properties of the HAP materials (refer to Fig. S1 in the Supplementary Information). Based on the concentration of Sr^{2+} in the supernatant, the sorption efficiency (A_{eff}) of DEF-HAP and ST-HAP was calculated as follows:

$$A_{eff}(\%) = 100 \times \left(1 - \frac{C}{C_0}\right), \quad (1)$$

where C_0 and C are the initial and final (after 5 h) concentrations (mg/L) of Sr^{2+}, respectively.

As shown in Fig. 2(a), DEF-HAP demonstrates a high A_{eff} in the absence of Mg^{2+} and Ca^{2+} (83%), and the values remain almost constant in the presence of Mg^{2+} and Ca^{2+} at concentrations between 0.1 and 1.0 mmol/L. The values decrease as the concentration increases above 1.0 mmol/L, decreasing to 42% for Mg^{2+} and 14% for Ca^{2+} at 50 mmol/L. Conversely, ST-HAP exhibits a lower A_{eff} than DEF-HAP in the absence of Mg^{2+} and Ca^{2+} (74%) and the values decrease even in the presence of small amounts of Mg^{2+} and Ca^{2+} (72% for Mg^{2+} and 51% for Ca^{2+} at 0.1 mmol/L). These values significantly decrease to 14% for Mg^{2+} and 0.5% for Ca^{2+} at 50 mmol/L. The dashed and solid lines in Fig. 2(a) and (b) denote the Mg^{2+} and Ca^{2+} concentrations in seawater and groundwater at FNPP, respectively. Our results demonstrate that DEF-HAP can maintain its Sr^{2+} sorption capacity under the existing groundwater conditions at FNPP.

Dependence on initial concentration. We investigated the dependence of the Sr^{2+} concentration on the sorption capacity of DEF-HAP and ST-HAP using aqueous solutions initially containing 0.01, 0.05, 0.1, 1, 5, and 10 mmol/L of Sr^{2+} at pH 7. Their supernatants were obtained after 5 h, and A_{eff} was estimated using Eq. (1). As shown in Fig. 3(a), the A_{eff} of DEF-HAP is 82% at 0.01 mmol/L; this value remains almost constant as the concentration is increased to 0.1 mmol/L. For higher Sr^{2+} concentrations, A_{eff} decreases with an increase in the concentration and decreasing to 10% at 10 mmol/L. For ST-HAP, the A_{eff} at 0.01 mmol/L is 70%, which significantly decreases above 0.05 mmol/L. The values of A_{eff} for DEF-HAP are higher than those of ST-HAP at all measured concentrations. The most significant difference was observed at 1 mmol/L where the value of A_{eff} for DEF-HAP was 60%, which is 75% higher than that of ST-HAP at the same concentration, that is, 15%.

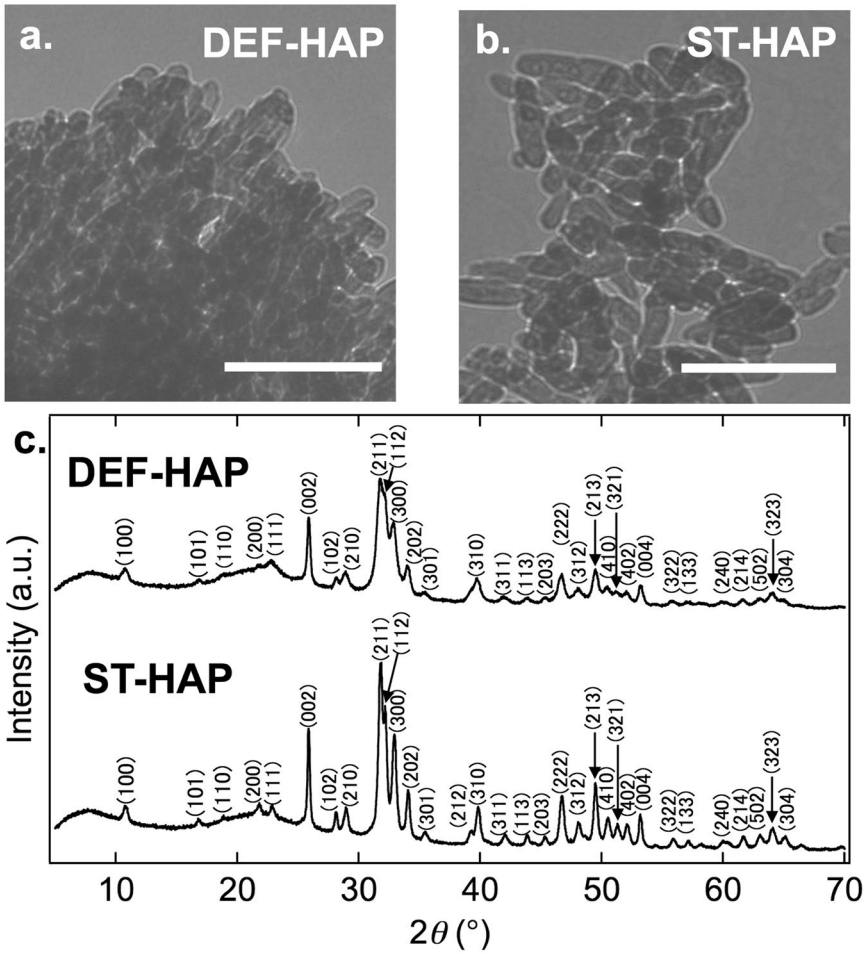

Figure 1. HAP crystal structures. Panels (a,b) show the TEM images of DEF-HAP and ST-HAP, respectively. The scale bars represent 200 nm. (**c**) X-ray powder diffraction profiles of DEF-HAP and ST-HAP. Miller indices corresponding to an hydroxyapatite phase ($(P6_3/m)$[24] are indicated.

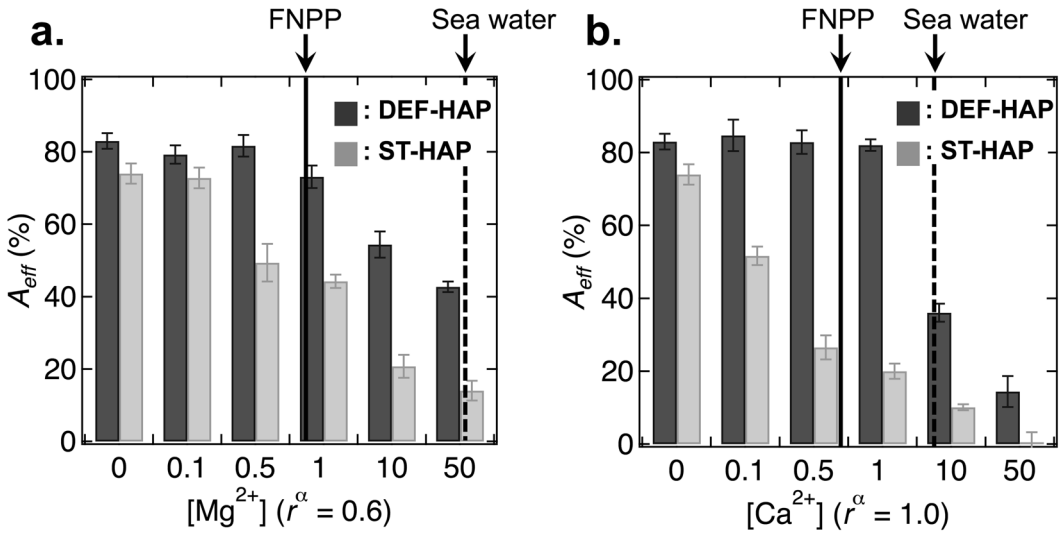

Figure 2. Effect of competing ions on the Sr^{2+} sorption capacity of HAPs. The change in A_{eff} for DEF-HAP (dark gray) and ST-HAP (light gray) as a function of the concentration (mmol/L) of (**a**) Mg^{2+} ([Mg^{2+}]) and (**b**) Ca^{2+} ([Ca^{2+}]) is shown. The dashed and solid lines represent the approximate average [Mg^{2+}] and [Ca^{2+}] in seawater[14] (52 mmol/L for Mg^{2+} and 9.4 mmol/L for Ca^{2+}) and in FNPP ground water[15] (0.86 mmol/L for Mg^{2+} and 0.70 mmol/L for Ca^{2+}), respectively. The hydrated ionic radii of Mg^{2+} and Ca^{2+} are 0.6 Å and 1.0 Å, respectively. α is the ionic hydrated radius (Å).

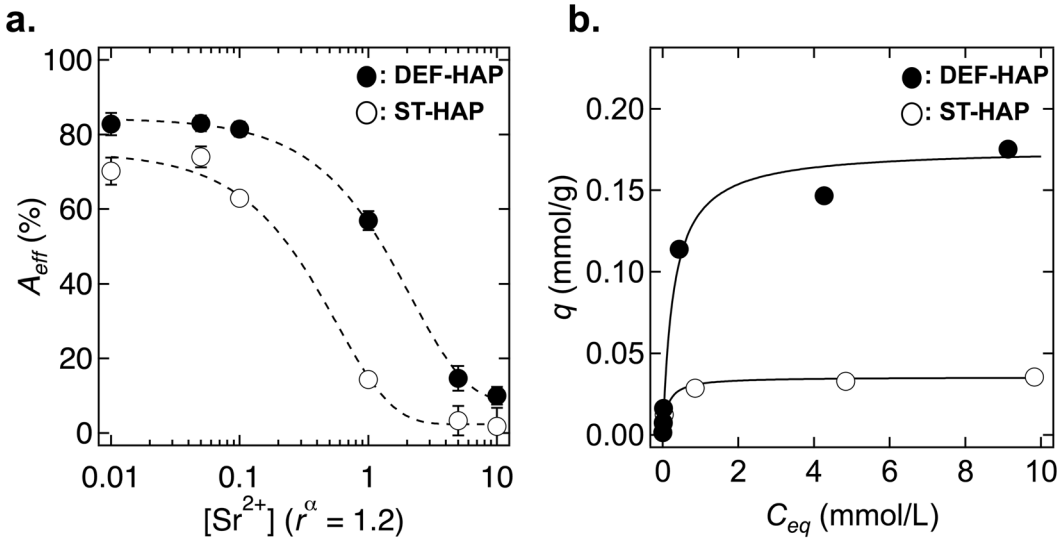

Figure 3. Dependence of initial concentration of Sr^{2+} on the sorption capacity of HAPs. (**a**) A_{eff} of DEF-HAP (closed circles) and ST-HAP (open circles) as a function of Sr^{2+} concentration ([Sr^{2+}]) between 0.01 and 10 mmol/L. The dashed lines are guides to the eye. The hydrated ionic radius of Sr^{2+} is 1.2 Å. α is the ionic hydrated radius (Å). (**b**) Sorption isotherm of DEF-HAP (closed circles) and ST-HAP (open circles) fitted to a Langmuir isotherm model using the values of q_{max} and b (solid lines) (refer to Fig. S2 in the Supplementary Information).

	R^2	q_{max} (mg/g)	b
HAP400	0.987	15.4	3.50
HAP100	0.981	3.11	7.70

Table 2. Langmuir isotherm parameters for DEF-HAP and ST-HAP.

Figure 3(b) shows the sorption isotherms of DEF-HAP and ST-HAP fitted to a Langmuir isotherm model[33]. The model assumes monolayer coverage on a surface with a finite number of identical sites and is represented as follows[33]:

$$\frac{C_e}{q_e} = \frac{1}{q_{max}{}^b} + \frac{C_e}{q_{\max}}, \tag{2}$$

where C_e is the equilibrium concentration (mg/L) of Sr^{2+}, q_e is the amount of adsorbed Sr^{2+} at equilibrium (mg/g), and q_{max} (mg/g; maximum sorption capacity) and b (affinity) are Langmuir constants, respectively. The parameters q_{max} and b, evaluated via Eq. (2) (refer to Fig. S2 in the Supplementary Information), and the coefficients of determination (R^2) are summarized in Table 2. The result shows that DEF-HAP (15.4 mg/g) has a larger maximum sorption capacity for Sr^{2+} than ST-HAP (3.11 mg/g).

Extended X-ray absorption fine structure (EXAFS) measurements. The Sr^{2+} sorption mechanism on DEF-HAP and ST-HAP was investigated via EXAFS measurements. Figure 4(a) and (b) shows the EXAFS spectra of DEF-HAP and ST-HAP around the *K*-edge of Sr and the Fourier transforms of DEF-HAP and ST-HAP at concentrations of 10 and 100 mmol/L of Sr^{2+} (these samples are referred to as DEF-HAP-Sr10, DEF-HAP-Sr100, ST-HAP-Sr10, and ST-HAP-Sr100). The features of the spectra are similar to those of a previously reported Sr-doped hydroxyapatite[22]. As shown in Fig. 4(b), three peaks (P_1, P_2, and P_3) are observed around r (interatomic distance) = 1.9, 2.8, and 3.8 Å for all samples. These peaks are attributed to two O shells and one P shell nearest to the Sr[22,34,35]. The EXAFS spectrum obtained for ST-HAP-Sr100 differs from that of the other samples as the P_1 peak shifts to a longer r, whereas P_2 shifts to a shorter r when ST-HAP is exposed to 100 mmol/L of Sr^{2+}; moreover, the peak intensity of P_3 decreases. The spectral line shapes of DEF-HAP are similar irrespective of the Sr^{2+} concentration.

Discussion

Sorption tests for HAPs in the presence of competing ions showed that the A_{eff} of both DEF-HAP and ST-HAP is affected less by Mg^{2+} than by Ca^{2+} (Fig. 2). Divalent cations can be exchanged with Ca^{2+} in crystals; moreover, ions with hydrated radii in the range of 0.9–1.3 Å are easily exchanged as compared with other ions[36]. Since the hydrated ionic radius of Sr^{2+} is 1.2 Å[23], sorption of Sr^{2+} might occur prior to that of Mg^{2+}, which has a hydrated ionic radius of 0.6 Å[23]. With Ca^{2+} as the competing ion, DEF-HAP maintains its A_{eff} for a specific range of concentrations. This means the Sr^{2+} sorption capacity of DEF-HAP is equal to or greater than its Ca^{2+} sorption capacity.

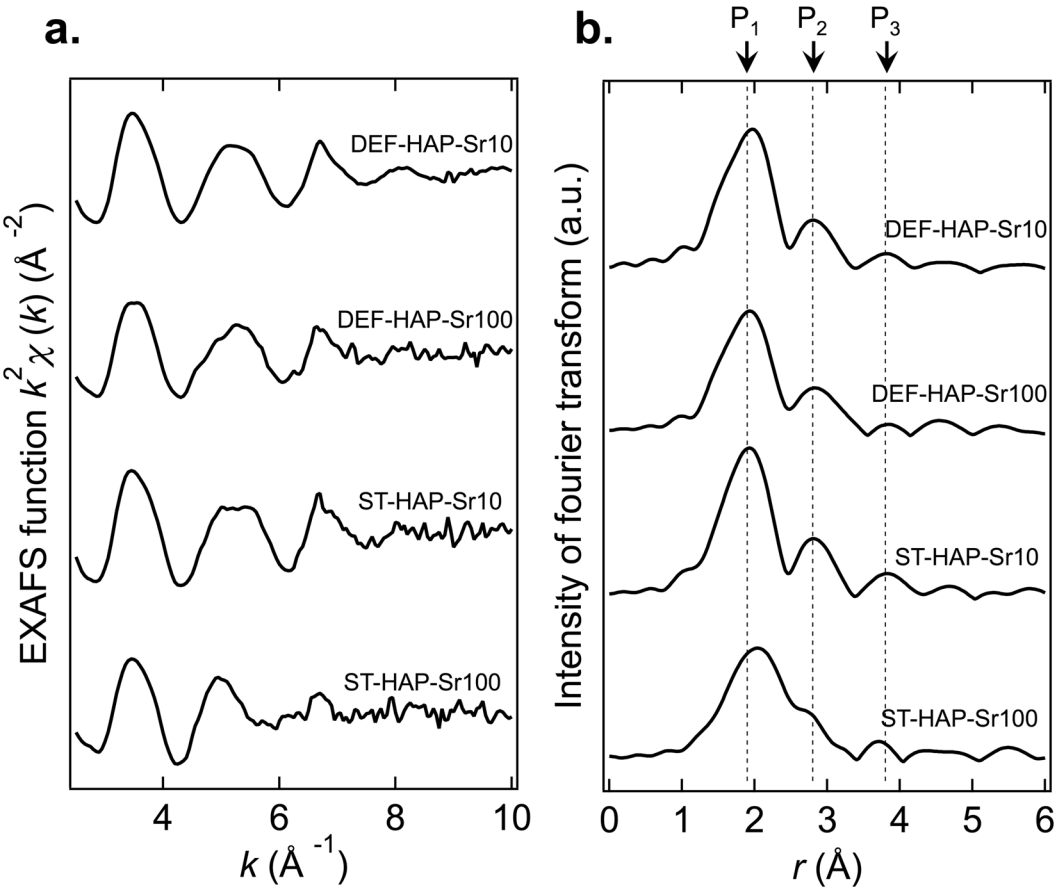

Figure 4. Sr *K*-edge EXAFS analysis of the HAP samples. (**a**) EXAFS spectra of DEF-HAP and ST-HAP exposed to 10 and 100 mmol/L of Sr^{2+}, where *k* is the wavenumber. (**b**) Fourier transforms of the EXAFS spectra where *r* is the interatomic distance. Notably, the *r* does not take phase shifts into account. Transforms were conducted with k^2 weighting. Three peaks (P_1, P_2, and P_3) are observed at around $r = 1.9$, 2.8, and 3.8 Å in all samples.

The result implies that the vacant Ca^{2+} sites in DEF-HAP are slightly larger than the ionic radius of Ca^{2+}, making them more suitable for Sr^{2+} than for Ca^{2+}.

The A_{eff} of DEF-HAP is higher than that of ST-HAP at all the tested concentrations, as shown in Fig. 3. The sorption of divalent cations onto HAPs occurs both at the surface and within the crystals[21]. In aqueous solutions, strontium mainly exists as Sr^{2+} at pH 7[37], and these positively charged species are actively adsorbed at the negatively charged sites in the HAPs by electrostatic attraction. Thus, the higher negative charge on the surface of DEF-HAP (zeta potential of −20.1 mV) compared with that on the surface of ST-HAP (zeta potential of −5.46 mV) contributes to its higher absorptivity of Sr^{2+}. The higher negative zeta potential of DEF-HAP might be due to the existence of PO_4^{3-}, OH^-, or HPO_4^- surface ions; similar observations have also been made for other Ca-deficient hydroxyapatites[38,39]. These results suggest that DEF-HAP has a higher Sr^{2+}-selective sorption capacity owing to its negatively charged surface and the vacant Ca^{2+} sites within its crystal structure.

In Fig. 4(b), EXAFS spectra of DEF-HAP for different Sr^{2+} concentrations appear to be independent of concentration, suggesting that the sorption sites of DEF-HAP remain unchanged for all the studied conditions; however, the ST-HAP spectra vary with the Sr^{2+} concentration. In the spectrum of ST-HAP-Sr100, P_1, which is related to the O shell nearest to the Sr, shifts to a larger *r*, indicating that there are two types of sites providing shorter and longer Sr–O distances in ST-HAP. This implies that one site providing a short Sr–O distance is occupied at a certain Sr^{2+} concentration below 100 mmol/L; moreover, the other site providing long Sr–O distance becomes more dominant in ST-HAP. The spectra for DEF-HAP suggest that DEF-HAP only contains sites that provide a shorter Sr–O distance, in which O strongly interacts with Sr^{2+}. This might contribute to the higher value of q_{max} observed in Fig. 3.

In conclusion, Sr^{2+} sorption tests in the presence of competing cations demonstrate that DEF-HAP has a higher Sr^{2+} sorption selectivity than ST-HAP even for conditions similar to those in the groundwater at FNPP. The difference in sorptivity for the competing cations indicates that the ionic radius is one of the important factors affecting the sorption of ions onto HAPs and that HAPs are efficient sorbents for Sr^{2+}, which has a hydrated ionic radius of 1.2 Å. Furthermore, DEF-HAP could maintain its Sr^{2+} sorption capacity even in the presence of Ca^{2+}. Compared with ST-HAP, DEF-HAP showed a higher A_{eff} for solutions with various Sr^{2+} concentrations. The EXAFS results demonstrate that compared with ST-HAP, DEF-HAP has significantly more sorption sites

where Sr^{2+} can be stably and preferentially sorbed. These results provide useful insights that may assist the future development of HAP-based sorption materials for ^{90}Sr by controlling their chemical composition.

Methods

Materials. Stoichiometric hydroxyapatite ($Ca_{10}(PO_4)_6(OH)_2$, Ca/P = 1.68, ST-HAP) and Ca-deficient hydroxyapatite ($Ca_{10-x}(HPO_4)_x(PO_4)_{6-x}(OH)_{2-x}$, Ca/P = 1.38, DEF-HAP) were supplied by Taihei Chemical Industrial Co., Ltd., Japan. ST-HAP was synthesized by mixing calcium hydroxide and phosphoric acid solutions[40,41]. The precipitate was dried at 100 °C. DEF-HAP was synthesized by mixing slurries of calcium hydrogen phosphate dihydrate with an aqueous solution of sodium hydroxide[31,41]. The precipitate was dried at 150 °C. Strontium chloride ($SrCl_2$), magnesium chloride ($MgCl_2$), and calcium chloride ($CaCl_2$) were purchased from Wako Pure Chemical Industries Co., Ltd., Japan. Sr standard solutions (1 mg/mL) for ICP-MS (PerkinElmer Japan Co., Ltd., United States) were also purchased from Wako Pure Chemical Industries. All materials were used without further purification.

Characterizations. XRD measurements were performed using an X-ray diffractometer (Ultima IV, Rigaku Co., Ltd. Japan) with Cu-K_α radiation ($\lambda = 0.15418$ nm) at room temperature. The sample was mounted on a glass plate and optically centered on the diffractometer. The diffraction data was collected in steps of 0.02° in for 2θ angles between 10° and 70°. TEM images of the HAP samples were obtained using a JEOL TEM (HT-7700, Hitachi, Tokyo, Japan) operated at an electron beam accelerating voltage of 100 kV. The zeta potentials of the HAP samples were measured at room temperature using a Malvern Zetasizer (Marvern Instruments Ltd., Worcestershire, UK). The unit automatically calculates the electrophoretic mobility of the particle and converts the electrophoretic mobility into a zeta potential using the Smoluchowski equation. One milligram of each HAP sample was dispersed in 1 mL of MilliQ water at pH 7 and stirred for 5 h. Each data point in the A_{eff} plots is an average of approximately three measurements. The pH of the suspension was adjusted using an aqueous solution of 0.1 mmol/L hydrochloric acid (HCl). The pH of the suspension was measured using a digital pH meter (Mettler Toledo Co., Ltd., Switzerland).

Sorption tests. The effect of competing ions on the Sr^{2+} sorption capacities of DEF-HAP and ST-HAP was investigated using $SrCl_2$, $CaCl_2$, and $MgCl_2$ solutions. We stirred 7 mL of aqueous solutions containing 35 mg of DEF-HAP or ST-HAP and Sr^{2+} (0.05 mmol/L) in MilliQ water for 5 h at room temperature in the presence of Ca^{2+} or Mg^{2+} at concentrations of 0.1, 0, 1, 10, or 50 mmol/L. The initial pH was adjusted to 7 using 0.1 mmol/L of HCl. Aliquots (1 mL) of the suspension were taken after 5 h and were centrifuged at 10,000 g for 5 min. The pH was maintained at 7 for this study since the groundwater at FNPP generally has a pH of 7. The supernatant was filtered through a 0.1-mm polyvinylidene difluoride (PVDF) filter (Millex-GV, Millipore Co., United States). The concentrations of Sr^{2+} in the supernatant were measured via ICP-MS (PerkinElmer Japan Co., Ltd., Japan).

To investigate the dependence of Sr^{2+} concentration on the sorption efficiency, 35 mg of DEF-HAP or ST-HAP was mixed with Sr^{2+} at concentrations of 0.01, 0.05, 0.1, 1, 5, 10, or 100 mmol/L for 5 h at room temperature. The supernatant was obtained after 5 h, and the sorption efficiency was estimated as aforementioned.

EXAFS measurements. EXAFS measurements were performed at the Sr *K*-edge on the BL14B1 line of SPring-8[42,43], where X-rays (~16,100 eV) were continuously generated from a bending magnet source. The incident X-rays were monochromatized by two silicon (311) crystals. For the measurements, powder samples were pressed into pellets and placed in the X-ray path. The absorption data were analyzed using the ATENA software package[44].

References

1. Yasunari, T. J. *et al.* Cesium-137 deposition and contamination of Japanese soils due to the Fukushima nuclear accident. *Proc. Natl. Acad. Sci* **108**, 19530–19534 (2011).
2. Steinhauser, G., Schauer, V. & Shouzugawa, K. Concentration of strontium-90 at selected hot spots in Japan. *Plos One* **8**(1–5), e57760 (2013).
3. Koarai, K. *et al*. 90Sr in teeth of cattle abandoned in evacuation zone: Record of pollution from the Fukushima-Daiichi Nuclear Power Plant accident, *Sci. Rep*. **6**, doi: 10.1038/srep24077 (1–9) (2016).
4. Povinec, P. P., Hirose, K., Aoyama, M. *Fukushima accident* 103–130 (Elsevier Inc., 2013).
5. Stephanie, H. S. *et al*. Influence of pH, competing ions, and salinity on the sorption of strontium and cobalt onto biogenic hydroxyapatite. *Sci. Rep* **6**(1–8), 23361 (2016).
6. Luning, K. G., Frolen, H., Nelson, A. & Ronnback, C. Genetic effects of strontium-90 injected into male mice. *Nature* **197**, 304–305 (1963).
7. Kubota, T., Fukutani, S., Ohta, T. & Mahara, Y. Removal of radioactive cesium, strontium, and iodine from natural waters using bentonite, zeolite, and activated carbon. *J. Radioanal. Nucl. Chem.* **296**, 981–984 (2013).
8. El-Kamash, A. M., El-Naggar, M. R. & El-Dessouky, M. I. Immobilization of cesium and strontium radionuclides in zeolite cement blends. *J. Hazard. Mater.* **136**, 310–316 (2006).
9. Merceille, A., Weinzaepfel, E., Barre, Y. & Grandjean, A. The sorption behavior of synthetic nonatitanate and zeolite A for removing radioactive strontium from aqueous wastes. *Sep. Purif. Technol.* **96**, 81–88 (2012).
10. IAEA. Application of Ion Exchange Processes for the Treatment of Radioactive Waste and Management of Spent Ion Exchangers. *Technical Reports Series No. 408* (International Atomic Energy Agency, 1994).
11. Lu, N. & Mason, C. F. V. Sorption-desorption behavior of strontium-85 onto montmorillonite and silica colloids. *Appl. Geochem.* **16**, 1653–1662 (2001).
12. Nishiyama, Y., Hanafusa, T., Yamashita, J., Yamamoto, Y. & Ono, T. Adsorption and removal of strontium in aqueous solution by synthetic hydroxyapatite. *J. Radioanal. Nucl. Chem.* **307**, 1279–1285 (2016).

13. Zhang, E., Kuraoka, Y. & Kumagai, M. Preparation of a novel macroporous silica-based 2,6-bis(5,6-diisobutyl-1,2,4-triazine-3-yl) pyridine impregnated polymeric composite and its application in the adsorption for trivalent rare earths. *J. Radioanal. Nucl. Chem.* **274**, 455–464 (2004).
14. Wajima, T. Ion exchange properties of Japanese natural zeolites in seawater. *Anal. Sci.* **29**, 139–141 (2013).
15. TEPCO. About the completion of the countermeasure work to address the downward flow of strontium present in the soil in relation to the leak in H4 area tank Available at: http://www.tepco.co.jp/en/nu/fukushima-np/handouts/2014/images/handouts_140911_05-e.pdf (Accessed: 1st February 2015) (2014).
16. Lin, Y., Fryxell, G. E., Wu, H. & Engelhard, M. Selective sorption of cesium using self-assembled monolayers on mesoporous supports. *Environ. Sci. Technol. Lett* **35**, 3962–3966 (2001).
17. Sangvanich., T. *et al*. Selective capture of cesium and thallium from natural waters and simulated wastes with copper ferrocyanide functionalized mesoporous silica. zed. *J. Hazard. Mater.* **182**, 225–231 (2010).
18. Dorozhkin, S. V. & Epple, M. Biological and medical significance of calcium phosphates. *Angew. Chem. Int. Ed.* **41**, 3130–3146 (2002).
19. Zhuang, Z. *et al*. Development of a, b-plane-oriented to a(b) –and c-axes. *Acta Biomater.* **9**, 6732–6740 (2013).
20. Hughes, J. M., Cameron, M. & Crowley, K. D. Structural variations in natural F, OH, and Cl apatites. *Am. Mineral.* **74**, 870–876 (1989).
21. Bazin, D. *et al*. The status of strontium in biological apatites an XANES/EXAFS investigation. *J. Synchrotron Rad* **21**, 136–142 (2014).
22. Terra, J. *et al*. The structure of strontium-doped hydroxyapatite: an experimental and theoretical study. *Phys. Chem. Chem. Phys.* **11**, 568–577 (2009).
23. Shannon, R. D. Revised effective ionic radii and systematic studies of interatomic distances in halides and chalcogenides. *Acta Cryst* **A32**, 751–767 (1976).
24. Bigi, A., Boanini, E., Capuccini, C. & Gazzano, M. Strontium-substituted hydroxyapatite nanocrystals. *Inorg. Chim. Acta* **360**, 1009–1016 (2007).
25. Vermeul, V. R. *et al*. An injectable apatite permeable reactive barrier for *in situ* 90Sr immobilization ground water. *Monit. R* **34**, 28–41 (2014).
26. Mori, K. *et al*. Controlled synthesis of hydroxyapatite-supported palladium complexes as highly efficient heterogeneous catalysts. *J. Am. Chem. Soc.* **124**, 11572–3 (2002).
27. Liou, S. C., Chen, S. Y., Lee, H. Y. & Bow, J. S. Structural characterization of nano-sized calcium deficient apatite powders. *Biomaterials* **25**, 189–196 (2004).
28. Brown, P. W. & Martin, R. I. An analysis of hydroxyapatite surface layer formation. *J. Phys. Chem. B* **103**, 1671–1675 (1999).
29. Moriguchi, T., Nakagawa, S. & Kaji, F. Adsorbability of alizarin reds on Fe(III) and Pb(II) treated hydroxyapatites in water. *Phosphorous Res. Bull* **22**, 62–72 (2008).
30. Moriguchi, T., Nakagawa, S. & Kaji, F. Reaction of Ca-deficient hydroxyapatite with heavy metal ions along with metal substitution. *Phosphorous Res. Bull* **24**, 54–60 (2010).
31. Nakagawa, S., Kaji, F., Yamagami, T., Sakurai, M. & Watanabe, T. Pb^{2+} ion removal ability of hydroxyapatite. *Phosphorus Res. Bull* **14**, 119–122 (2002).
32. Sheha, R. R. Sorption behavior of Zn(II) ions on synthesized hydroxyapatites. *J. Colloid. Inter. Sci* **310**, 18–26 (2007).
33. Langmuir, I. The adsorption of gases on plane surfaces of glass, mica, and platinum. *J. Am. Chem. Soc.* **40**, 1361–1403 (1918).
34. Harries, J. E., Hukins, D. W. L., Holt, C. & Hasnain, S. S. Conversion of amorphous calcium phosphate into hydroxyapatite investigated by EXAFS spectroscopy. *J. Cryst. Growth* **84**, 563–570 (1987).
35. Rokita, E., Hermes, C., Nolting, H. F. & Ryczek, J. Substitution of calcium by strontium within selected calcium phosphate. *J. Cryst. Growth* **130**, 543–552 (1993).
36. Suzuki, T., Hatsushika, T. & Miyake, M. Synthetic hydroxyapatites as inorganic cation exchangers. *Part 2, J. Chem. Soc. Faraday Trans.* **1**, 3605–3611 (1982).
37. Cole, T., Bidoglio, G., Soupioni, M., Gorman, M. O. & Gibson, N. Diffusion mechanisms of multiple strontium species in clay. *Geochim. Cosmochim. Acta* **64**, 385–396 (2000).
38. Himeno, KimH. M., Kawashita, T., Kokubo, M. & Nakamura, T. T. The mechanism of biomineralization of bone-like apatite on synthetic hydroxyapatite: an *in vitro* assessment. *J. R. Soc. Interface* **1**, 17–22 (2004).
39. Ducheyne, P., Kim, C. S. & Pollack, S. R. The effect of phase differences on the time-dependent variation of the zeta potential of hydroxyapatite. *J. Biomed. Mater. Res.* **26**, 147–168 (1992).
40. Matsuda, N., Kaji, F., Nakagawa, S., Uemura, T. & Watanabe, M. Thermal changes of carbonate-containing hydroxyapatite. *Inorganic Materials* **5**, 398–404 (1998).
41. Nakagawa, S., Yamagami, T., Kaji, F., Matsuda, N. Absorbents. Japan patent JP2003–126687A (2003).
42. Matsumura, D. *et al*. Dynamic structural change of Pd particles on LaFeO3 under redox atmosphere and CO/NO catalytic reaction studied by dispersive XAFS. *J. Phys. Conf. Ser.* **190**(1–7), 012154 (2009).
43. Tsuji, T. *et al*. Local structure around cesium in montmorillonite, vermiculite and zeolite under wet condition. *Clay Sci* **18**, 93–97 (2014).
44. Cervenka, V. *et al*. ATENA program documentation, theory and user manual, Cervenka Consulting. Prague (2005).

Acknowledgements

This work (author Y.S.) was partially supported by JSPS KAKENHI Grant JP16K21604 and JST initiatives for Atomic Energy Basis and Generic Strategic Research. A part of this study was conducted under the approval of Spring-8 (No. 2016A3611). The HAP samples were kindly supplied from Taihei Chemical Industrial Co., Ltd., Japan.

Author Contributions

Y.S. and R.M. wrote the manuscript. Y.S., R.M., N.K., and T.O. supervised the project. Y.S., N.K., D.M., T.T., R.K., and K.A. conducted experiments. All authors contributed to data analysis and manuscript reviewing.

Additional Information

Supplementary information accompanies this paper at doi:10.1038/s41598-017-02269-z

Competing Interests: The authors declare that they have no competing interests.